

Ganna Pirnach^{1*}, Taras Belyi², Vitalii Shpyg¹, Sergiy Dudar¹

¹Ukrainian Hydrometeorological Institute, Kyiv, Ukraine

²Institute of Geophysics, NAS of Ukraine, Kyiv, Ukraine

1. INTRODUCTION

Heavy precipitation is one of the dangerous natural phenomena (especially in mountain districts) which are observed on the territory of Ukraine. The amount of precipitation and their arising frequency depend not only on time of year, character of synoptic processes but also from the local features of territory and its relief. Ukrainian Carpathians are one of the most dangerous in this relation territory, where heavy and prolonged precipitation can be, and amount of precipitation to achieve over 200 mm per 12 hours (Boyko, 1999; Pirnach, 2002). In mountain regions such precipitation can be accompanied by fast floods' formation and torrents. These phenomena cause to damage to property and some times to victims. For example, damages of Transcarpathian (Zakarpatskiy) region of Ukraine from catastrophic floods in 1998 and 2001 amounted \$233.4 and \$55.3 millions respectively. Timely warning about such precipitation has a big practice sense. So, anyone information about reasons and mechanisms of their formation has very scientific importance. Unfortunately, heavy precipitation is investigated insufficient and their forecasting is not so good.

The processes of formation of precipitation in all times came into notice of many researchers through their deciding value in life of people, significance and complication of processes which determine them. The complete mathematical reflection of processes of formation of clouds and precipitation requires the common decision of equations, which describe the evolution of separate clouds' particles and particles of precipitation, conduct of aggregate of these particles, dynamics and thermodynamics of separate cloud, cloudy bands, all frontal cloudy system. Progress in development of calculable mathematics and technique did possible the decision of tasks, which was before

considered unattainable. The compatible modeling of the stratiform and convective clouds of the summer time frontal systems, which are often formed within the limits of one front as formations with spatial scales from hundreds of meters to hundreds of kilometers, belongs to such tasks. The examples of such modeling without taking into account relief of locality are resulted in (Pirnach, 2008). Plugging of topography in the developed models considerably complicates physical processes and requires development of different methods of decision depending on the put tasks. Modeling of heavy precipitation which was observed above Ukrainian Carpathians in transitional periods, with development of the special algorithms taking into account topography, able to regulate correlation between precipitation of thundershowers and of longtime precipitation with predominance of the stratified cloudiness was offered in (Pirnach et al., 2006; Pirnach, 2007).

In this article basic attention was concentrated on the role of microphysical characteristics in formations of heavy precipitation, the evolution of which is determined with a great extent by the initial distributions of dynamic and microphysical features of the cloud systems. Numerical investigation has been conducted of conditions of atmospheric precipitation formation above Ukraine during synoptic period from 21 to 27 of July 2008 while strong floods in the Eastern Carpathians in detail. Series of numerical experiments have been carried out with different relationships between ice particles and drops. Relationships varied by including or excluding from calculations of different mechanism of cloud and precipitation formation.

2. RESEARCH METHODOLOGY

2.1 Basic foundations

Investigation of the fields of frontal precipitation of different physical nature was carried out by the 3-D diagnostic and forecasting models of the frontal systems. Data got by diagnostic models, used as initial for the study of evolution of cloudiness and precipitation taking

*Corresponding author address: Ganna M. Pirnach, Ukrainian Hydrometeorological Institute, Dept. of the Atmosphere Physics, Kiyv, Ukraine, 03028; e-mail: hanna@uhmi.org.ua.

into account the different mechanisms of precipitation formation. For modeling of cloudiness cells with different spatial scales the nested grids were used in numeral models.

Atmospheric front formation, its development in time and space was modeled by integration of the system of equations, which included equations for air motion, water vapor content, temperature transfer, the continuity and thermodynamic state equations. Additional integro-differential equations for the supersaturation with respect to water and ice were used. Cloud microphysics is considered explicitly by solving the kinetic equations for the droplet and crystal size distribution. The size distribution function of the cloud and precipitation particles is formed due to cloud condensation nucleation, ice nucleation, growth (evaporation) by deposition, and freezing, riming, collection by raindrops of cloud drops. Droplet and ice nucleation is accounted by parameterization in the 3-D forecasting model.

To study the mesostructure of the atmospheric fronts it is necessary that meteorological data are collected to identify changes on the mesoscale of tens of kilometers. In Ukraine rawinsonding stations are hundreds kilometers apart. Naturally, to these data it is possible to add aircraft, radiolocation data and so on. Usually such data are received irregularly and from different points of the investigated space. The necessary data, at the points of regular grid with the grid spacing about ten kilometers, may be obtained by using the finite-difference system of equations. The semi-empirical 3-D diagnostic model of the front saws used for describing of fields of meteorological elements at a fixed time in a fixed area. The full details may be found in Pirnach and Krakovskaya (1994) and in Pirnach (2008).

2.2 Description of 3-D forecasting model

σ -Z coordinate system (Kasahara, 1974) is used in the model. This system allows taking into account a relief forms and keeping permanent height of plane which limited the area of integration from above. In diagnostic models the account of topography was carried out as follows. At first the fields of meteorological elements were built in the Cartesian coordinate system without topography, as in (Palamarchuk, 1992). Then the redistribution of unknown values was conducted in σ -Z coordinate system grid points by interpolation. New coordinates can be written as following:

$$\xi = x, \quad \eta = y, \quad \zeta = \frac{z - \Gamma}{H - \Gamma} H,$$

where x, y, z are Cartesian coordinates; ξ, η, ζ are σ -Z topographical coordinates; $\Gamma(x, y)$ is a relief function; H is a Z-maximum. For the modeling of evolution of mesoscale cloud systems in time and space the equations system was used in such form:

$$\frac{dS_i}{dt} = F_i + \Delta S_i, \quad (1)$$

$$\frac{\partial \rho u}{\partial \xi} + \frac{\partial \rho v}{\partial \eta} + \frac{\partial \rho \bar{w}}{\partial \zeta} = 0, \quad (2)$$

$$\rho = \frac{P}{RT}, \quad (3)$$

$$S_i = (u, v, \bar{w}, T, q, f_k), \quad (4)$$

$$i = 1, 2, \dots, 8, \quad k = 1, 2, 3,$$

$$\frac{d}{dt} = \frac{\partial}{\partial t} + u \frac{\partial}{\partial \xi} + v \frac{\partial}{\partial \eta} + \bar{w} \frac{\partial}{\partial \zeta}, \quad (5)$$

$$\Delta S_i = k_\xi (S_{\xi\xi} + S_{\eta\eta}) + k_\zeta S_{\zeta\zeta}, \quad (6)$$

$$F_1 = lv - \frac{1}{\rho} \left[\frac{\partial p}{\partial \xi} - \rho g G_1 \right], \quad (7)$$

$$F_2 = -lu - \frac{1}{\rho} \left[\frac{\partial p}{\partial \eta} - \rho g G_2 \right], \quad (8)$$

$$F_3 = -g - \frac{1}{\rho} \left[\frac{\partial p}{\partial \xi} \frac{1}{G_0} \right], \quad (9)$$

$$F_4 = \sum_{k=1}^3 \alpha_k \varepsilon_k + \alpha_p \frac{dp}{dt}, \quad (10)$$

$$F_5 = -\sum_{k=1}^3 \varepsilon_k, \quad (11)$$

$$F_6 = -\frac{\partial}{\partial r} \left(r_1 f_1 \right) + \frac{\partial f_1}{\partial \zeta} \frac{v_1}{G_0} + \quad (12)$$

$$+ I_a - I_{f1} - (c_{21} + c_{31}) f_1$$

$$F_7 = -\frac{\partial}{\partial r} \left(r_2 f_2 \right) + \frac{\partial f_2}{\partial \zeta} \frac{v_2}{G_0} - \quad (13)$$

$$- I_{f2} - \frac{\partial}{\partial r} \left(r_{c21} f_2 \right),$$

$$F_8 = -\frac{\partial}{\partial r} \left(r_3 f_3 \right) + \frac{\partial f_3}{\partial \zeta} \frac{v_3}{G_0} - \frac{\partial}{\partial r} \left(r_{c31} f_3 \right) + I_s + I_{f1} + I_{f2}, \quad (14)$$

where

$$\tilde{w} = \frac{G_1 u + G_2 v + w}{G_0}, \quad G_0 = 1 - \frac{\Gamma}{H}, \quad (15)$$

$$G_1 = \Gamma_x \left(\frac{\xi}{H} - 1 \right), \quad (16)$$

$$G_2 = \Gamma_y \left(\frac{\zeta}{H} - 1 \right).$$

$$\alpha_k = \frac{L_k}{c_p}, \quad (17)$$

$$\alpha_p = \frac{c_p - c_v}{c_p R \rho}.$$

t is time; r is radiuses of cloud and precipitation particles; u, v, w are wind velocity components across x, y, z axis, which are directed on east, north and perpendicular to the ground surface respectively; u, v, \tilde{w} are wind velocity components across ξ, η, ζ axis; ρ is air density; p, T are air pressure and temperature; q is specific humidity; l, g are the Coriolis parameter and free-fall acceleration, respectively; R is gas constant of dry air; c_p и c_v are the specific heat at constant pressure and the specific heat at constant volume of dry air, respectively; f_k are cloud particle size distribution functions (small drops, raindrops and crystals); L_k is are the condensation ($k= 1$) or sublimation ($k= 2$) heats, F_i are describes separate physical processes: $F_1 - F_3$ represent right parts of wind velocity projections, which included Coriolis parameter, free-fall acceleration, pressure gradients and etc.; $F_4 - F_5$ describe heat and moisture fluxes; $F_6 - F_8$ represent processes of droplets and crystal nucleation, cloud and precipitation particles falling velocities, their transfer, condensation and coagulation processes etc. Functions I_a, I_s, I_{f1}, I_{f2} describe of nucleation processes (generation on the cloud

condensation nuclei, ice nuclei, cloud droplets and precipitation drops, respectively). \dot{r}_{cik} and c_{ic} describe coagulation growth rate; Γ_x, Γ_y are first-order derivative of Γ by x and y . k_ξ, k_ζ are horizontal and vertical coefficients; ΔS_i is turbulent transfer, $S_{\xi\xi}, S_{\eta\eta}, S_{\zeta\zeta}$ are second-order derivative of functions by ξ, η, ζ , respectively.

2.3 The scheme of resolving of system of equations

The solution of the system is based on the splitting method (see Pirnach, 1994). In this work algorithm of vertical motions' calculation was substantially modified. Since convective formations (with which precipitation were connected) were very powerful, the domain top was increased to 15 km height. This led to additional problems during calculation of atmospheric processes near tropopause. Therefore, in the process of calculation, the area of integration was broken up on separate layers by height depending on speed of growth of vertical motions and location relatively to tropopause. This question requires separate consideration and in this work, devoted microphysical effects, it will not be examined.

A numerical algorithm which was used for integration of equations' system in partial derivative consisted from chain of finite-difference schemes, for each of these the method of decision was developed. The primary system of equations was broken on five subsystems which represented separate physical processes.

The first system described the processes of transfer of air and cloud particles and processes of initiation of particles on the condensation nuclei and on ice nuclei; second described processes which conditioned by pressures gradients; third are processes which conditioned inertias forces; fourth are processes of condensations; fifth are processes of coagulation. For example, the algorithm of coagulation processes calculation will be shown, because they have crucial role in precipitation formation in cumulus clouds. Coagulation processes were calculated in approaching of continuous growth. For calculation of drop fraction two equations for large and small drops solved separately:

$$\frac{\partial f_k}{\partial t} = -c_{nk} f_k \quad (18)$$

$$\frac{\partial f_n}{\partial t} = - \frac{\partial (r_{c_{nk}} f_n)}{\partial r}; \quad (19)$$

$$r_{c_{nk}} = \frac{\rho_k \rho \pi}{3 \rho_n r_n^2 K_{1n}} \times \int_0^{R_k} E(r_n + r_k)^2 (v_n - v_k) r_k^3 f_n dr; \quad (20)$$

$$c_{nk} = \pi \rho \int_{R_k}^{R_n} E(r_n + r_k)^2 (v_n - v_k) f_n dr. \quad (21)$$

Where $\kappa = 1$; $n = 2, 3$; n is number of fractions of precipitation particles (raindrops and crystals); k is number of cloud fraction (droplets); v_n and v_k are falling speed of small and big particles, calculated by Krystanov-Shmidt equation; K_{1n} is a coefficient of form, accepted equal 1; R_k , R_n are maximal radiuses of shallow and large particles, respectively, which take part in coagulation.

The coefficient of coagulation of large drops with shallow E was calculated by following equation:

$$E = E_0 \left[1 - \frac{r_2 r_m^3}{4 r^2 (r_2^2 - r^2)} \right]^2, \quad (22)$$

where r_2 is radius of large drop, $r_m = 14.5 \mu\text{m}$. Excepting of special experiments $E = 1$ for ice particles and $E_0 = 1$ for drops. For integration of equation (18) the implicit finite-difference scheme was used:

$$f_k^{j+1} = \frac{f_k^j}{1 + t_s c_{nk}}, \quad (23)$$

t_s is a time-step of integration. Since numerical experiments shown that the important role in heavy precipitation formation belongs to condensation processes, especially in large drop fraction, let's reduce scheme for calculation of these processes:

$$\frac{\partial f_i}{\partial t} = - \frac{\partial (f_i r_i)}{\partial r}; \quad (24)$$

$$\frac{\partial f_k}{\partial t} = - \frac{\partial (f_k r_k)}{\partial r}$$

$$\text{if } \dot{r}_m > 0, \quad \frac{(f_m^{j+1} - f_m^j)}{t_s} + \dot{r}_m \frac{(f_m^{j+1} - f_{m-1}^{j+1})}{\Delta r_m} + f_m^{j+1} \frac{(\dot{r}_{m+1}^{j+1} - \dot{r}_m^{j+1})}{\Delta r_{m+1}} = 0, \quad (25)$$

$$\text{if } \dot{r}_m < 0, \quad \frac{(f_m^{j+1} - f_m^j)}{t_s} + \dot{r}_m \frac{(f_{m+1}^{j+1} - f_m^{j+1})}{\Delta r_{m+1}} + f_m^{j+1} \frac{(\dot{r}_m^{j+1} - \dot{r}_{m-1}^{j+1})}{\Delta r_m} = 0. \quad (26)$$

In most cases, excepting the special calculations on the particles' spectrum study the growth rate of drops and crystals was calculated by Maxwell equation:

$$r_i = \frac{D \rho \Delta_i}{\Gamma_i \rho_i r}, \quad (27)$$

D is molecular diffusion coefficient; Γ_i is multiplication factor, which take into account differences between drop temperature and air temperature; Δ_i is water and ice supersaturation; ρ_i is water and ice density; ρ is air density; r is radius of particle; Δr is size drop interval. The indexes i , k , m present condensation on particles ($i = 1$ for cloud droplets; $i = 2$ for raindrops; $i = 3$ for ice crystals), coagulation growth for raindrops ($k = 2$) and ice crystals ($k = 3$) and number point by radii ($m = 1, 2, \dots$). For simplicity of description the number of functions skipped in Eqs. (24), (25). For more detail see Pirnach (1998).

Accordingly to Eq. (27), r_i decreases in inverse proportion to the radius of particle and must aspire to zero at radius aspiring to endlessness. If a numerator in Eq. (26) is the limited value, then approximation errors by Eq. (25) we can write in next form:

$$\delta = o(t_s) + o(\Delta r)^2 \pm \frac{1}{2} (\dot{r}_m f_{mrr} + f \dot{r}_{mrr}) \Delta r.$$

At a permanent step by radius the last member in this equation sets equal to zero. When the variable step by radius is used, the

approximation errors are proportional to step. It can result in piece spreading of spectrum. Probably, more rationally it would be to ignore condensation growth of raindrops, what was done in most cases, except for the special calculations. Especially, when Δ_1 aspires to zero and radius tend to infinity we have uncertainty with next type $\frac{0}{\infty}$ from the mathematical standpoint. It can result in unforeseen results, including to the collapse of calculation. But to unlimited growth of large drops the unlimited growth of water saturation can lead in certain terms too. It is possible, for example, if conditions of permanent influx of vapor to the set point and in disadvantage of particles of condensation nuclei or their lack. Getting in such terms, a drop is capable to the unlimited growth. At the prolonged existence of such condition clouds' areas of heavy precipitation formation can appear.

The initial values of drops' and crystals' distribution by size were set equal to zero or were calculated with the help semi-empirical functions. In most cases for calculation of the cloud particles distribution famous Khrgian-Mazin equation was used in the next form:

$$f_i = Ar^2 \exp(-Br),$$

$$A = 1,45q_i / r_m^6, \quad B = 3 / r_m,$$

where q_i is specific water content ($i = 1$) or ice content ($i = 2$); r_m is mean radius of cloud particles. It was assumed, that cloud particles are possessed in areas with ice saturation only. The values of q_1 and q_2 , which are included for calculation of A , were set proportional to the values of ice saturation. If ice saturation was not found in grid point, distribution of cloud particles $f_i = 0$. In most results of calculation of this work the proportional coefficient was equivalent to 5.

In separate cases the distribution of precipitation particles by size was set too. With this aim Marshall-Palmer distribution was used in such form:

$$f_i = f_0 \exp(-c_0 r).$$

where c_0 and f_0 are parameters (Marshall, 1948; Pirnach, 2007; Pirnach, 2008). In this work $c_0 = 1 \text{ cm}$, $f_0 = 0.001(\text{g}\cdot\text{cm}\cdot\text{s})^{-1}$.

3. WEATHER CONDITIONS JULY 21-28, 2008

On the 21th of July 2008 the weather situation above Europe was characterized by presence of two coupled cyclones above Scandinavian Peninsula. Thus in western from

they that disposed above the North Sea and Norway the surface center coincided practically with a height center (AT-500). This denotes that it was filled gradually (see Fig. 1, Fig. 2). Western air flow dominated above Central and East Europe. The low cyclone appeared in the area of divergence of isohypses above Pannonian Plain (see Fig. 3). The wide area of precipitation with thundershowers, hail and thunderstorms was stretched out from Scandinavian Peninsula to the north coast of the Adriatic Sea. During a day it had spreading to east. The high pressure area was dominated over the South of Ukraine and Asia Minor. At night on the 21th of July the circulation changed from quasi-latitudinal on meridional above greater part of Europe. Cold air flowing in warm and rich on moisture the Mediterranean region entailed forming of cyclone over Southern Italy. Its moving to the north-west was accompanied thundershowers and thunderstorms above Italy, countries of the Balkan Peninsula, Romania and Bulgaria. In the evening on the 22th of July the weather of western regions of Ukraine was stipulated by north-eastern cyclonical periphery and this cyclone pulled in its circulation moist air masses, which was formed above the Mediterranean and Black Seas. This created favorable terms for development of convection and fall of precipitation with thundershower character. The cyclone was a high baric formation (and traced on AT-500) and disposed within the bounds of U-similar pressure trough. The axis of which passed from Scandinavian Peninsula to the Ionian Sea. On 200 hPa height there was a powerful jet-stream which had orientation from the North Sea to Germany farther to Balearic Islands, Italy and southern part of Ukraine. In this flow wind speed hesitated within 30-50 m/s. On the 23th of July its displacement in common direction on east and considerable strengthening wind speed (to 60 m/s) especially above Balkan had place. The area with precipitation extended considerably above territory of Western and Central Europe and didn't displace practically to the east from Carpathians. During July, 23-25th the high cyclone was above territory of the Balkan Peninsula, Hungary and Romania. For three days its moving was enough insignificant with common direction on the north-east. This is related to the presence of powerful pressure ridge (which were traced clear on the absolute topography charts) from Gibraltar to Scandinavian Peninsula and from Plateau of Iran to the Western Siberian lowland. Thunderstorms and heavy shower were observed over all Central Europe and in Carpathians. On the north of Europe, in Germany and on the north-east of European part of Russia there was light

precipitation. In the morning on July, 26 the ridge of high pressure dominated above greater part of Europe. However, much countries of Balkan region, part of territory of bordering to its countries and East Europe were under cyclone influence, the height center of which was above Romania. Showers and thunderstorms were observed not only within frontier of this atmospheric formation but also in north-west direction from it (within the borders of baric saddle) and over the north of European part of Russia. Here the high cyclone disposed which was traced clear on AT-500 surface. On July, 27 the strengthening of anticyclone was occurred in the north of Europe. Here pressure was 1028.9 hPa against 1026.3 hPa in previous day. It moved in common direction from north-west on southeast. The pressure trough and Balkan cyclone were driven back considerably to east. The frontal systems relocated in the same direction. The jet-stream was oriented from the north of Turkey through the Black Sea and Sea of Azov on the Caspian Sea and Aral Sea. There wind speed amounted 40-50 m/s. On the 28th of July 2008 Ukraine was under influence of the meridional oriented trough yet, however above greater part of Europe the anticyclone was disposed. The continuous area of precipitation was observed in the north of Russia and over territory of Finland. In this day precipitation had local character and was insignificant. Practically all this time (from 22th to 27th of July) over the Black Sea near surface accordingly to the data of objective analysis of GFS (interpolated on more detailed grid with the help numerical mesoscale atmospheric model WRF ARW v.2.2.1) there was the low pressure area.

With the purpose of representing of precipitation distribution in space and time it was used WRF ARW v.2.2.1 (see Fig. 4). It enabled with the certain accuracy evenly (with a permanent horizontal step) represent position of precipitation lines and cores at the different moments of time. As we can see (Fig. 4) in the period which was considered, precipitation covered enormous territory above Balkan, Pannonian Plain and Carpathians with maximums over territory of Ukraine, Romania, Hungary and Moldova. Observed precipitation amount from surface hydrometeorological network shown on Fig. 5. It should be noted when in Zakarpatskiy and Chernivetskiy

Dates were shown on OX axis. Daily sums of precipitation (mm/24hour) are founded on OY. The name of station is written under chart.

regions precipitation fall didn't have expressed maximum evidently or them there was a few, over alpine part of Ukrainian Carpathians and over Prykarpattya the maximal values of daily sums of precipitation were

observed on July, 24-26. On the same territory the maximal amount of precipitation fell out during all period.

This case of heavy and prolonged precipitation had another feature. Already on the night of 21 on July 22 atmospheric front with the waves were observed over Europe and North Africa, respectively. The length of each of them was more than a thousand kilometers. Southern front with the waves stretched from the Atlantic coast of Africa to China. During March 22-23, 2008 the distance reduced considerably between them over Central and Eastern Europe. But the next day continuous wave structure of the southern front with the waves collapsed. Northern front with the waves has moved east, but has maintained its structure. During July 25-26 atmospheric fronts moved gradually to northeast and on the 27th of July they were already to eastward of Kyiv. The parallel structure between them remained roughly along latitude Kharkiv–Aktyubynsk. Accordingly to the synoptic charts here were observed not only light precipitation, but and showers (especially, on the section “warm front in the south – cold in the north”).

4. NUMERICAL SIMULATION OF CLOUD AND PRECIPITATION EVOLUTION

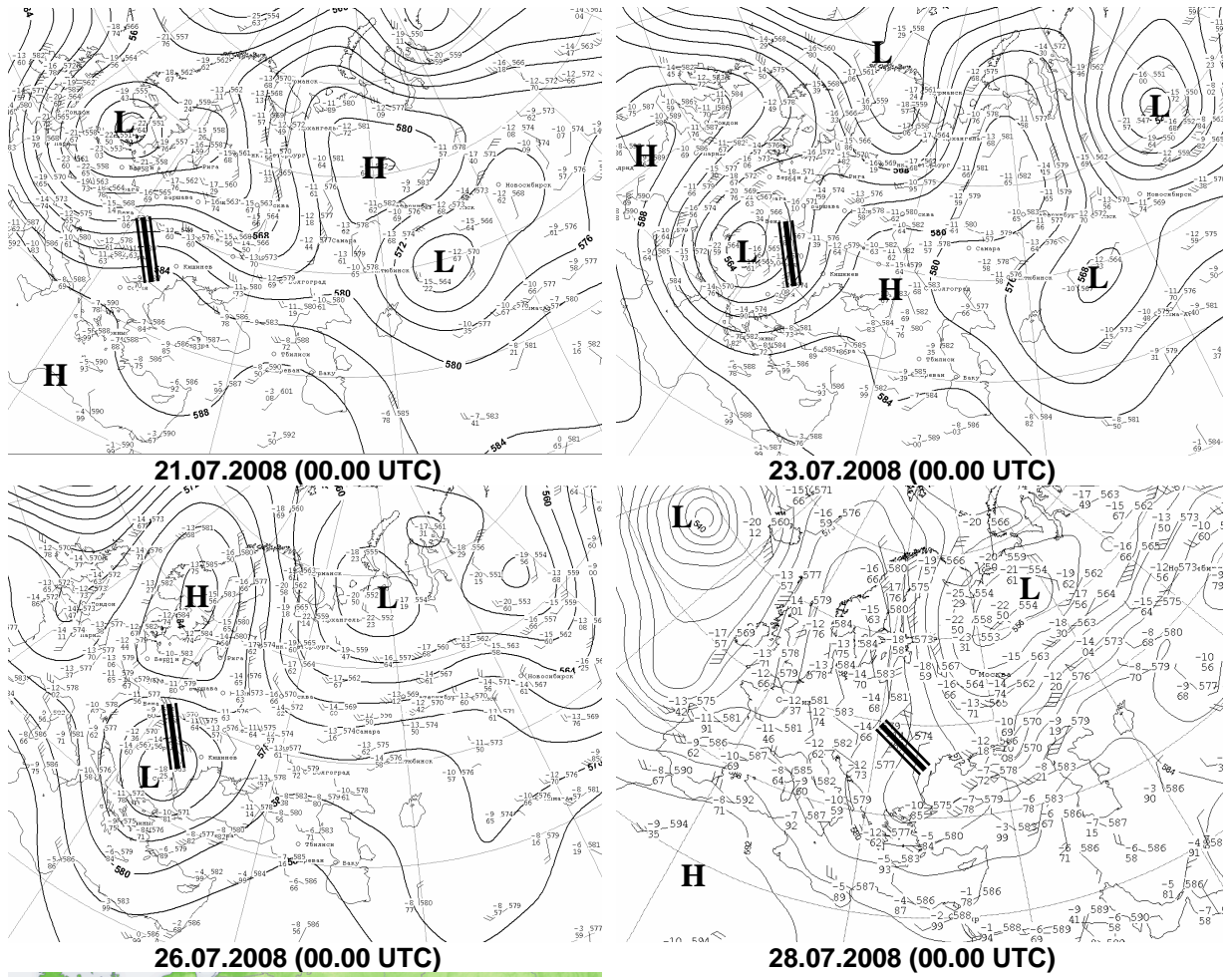
Fig. 6 displays the powerful convective formations that caused cells of heavy precipitation. These clouds have been calculated by integration of system (1). Initial condition can be obtained at $t = 0$ (23 30 UTC of 21 July) and $t = 0$ (23 30 UTC of 22 July).

They characterized by ice tops, mixed and ice supersaturation layers under. and by both strong updrafts and downdrafts that reaching 10 m/sec sometimes.

Such vertical motion is rare event but it clearly point out the possibility of the catastrophic precipitation. Many researches have been given the attention to a special role of ice tops in formation of catastrophic precipitation (Shyshkin, 1964). In this research the tops with the highest ice concentration had the key influence on precipitation intensity in the night from 22 to 23 July, 2008.

Influence of these ice tops was amplified by the high clouds (about 15 km) that contained the high concentration of small crystals that permanently seeded the mixing layers under.

Regions with ice supersaturation and strong updraft motion coincided rarely. This is due to a difference between motion speed of cloudy system and their separate parts. It did not exclude the possibility of precipitation in the nearly located supersaturation masses.



**Carpathian region.
Schematic orientation of
ridges over Ukraine and
Northern Romania**

FIG. 1. Charts of absolute topography and investigated region.
The date and time are shown under each from charts of absolute topography.

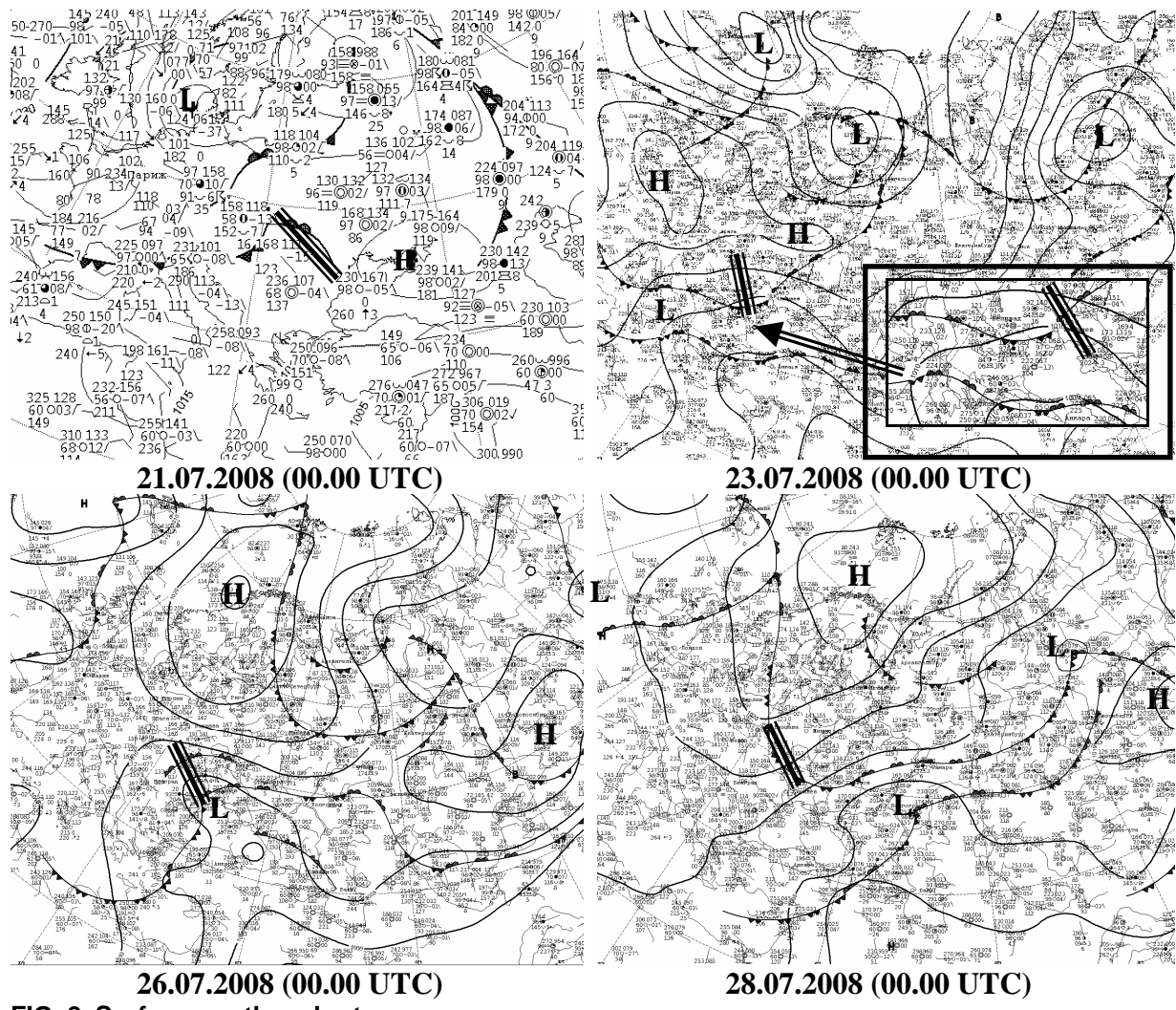
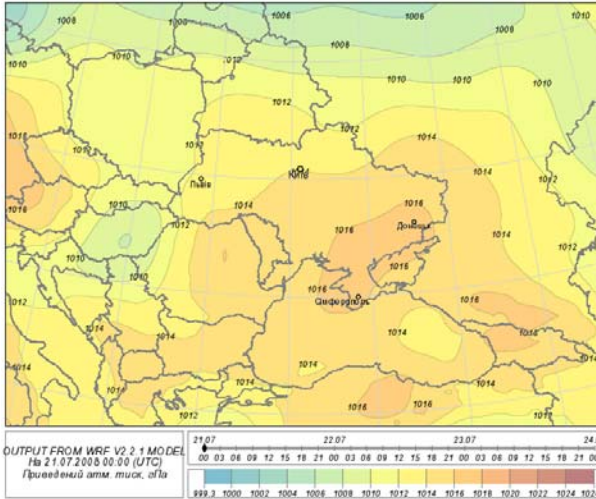
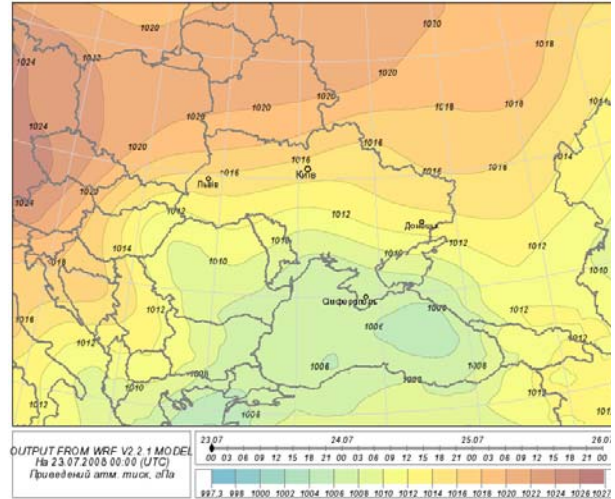


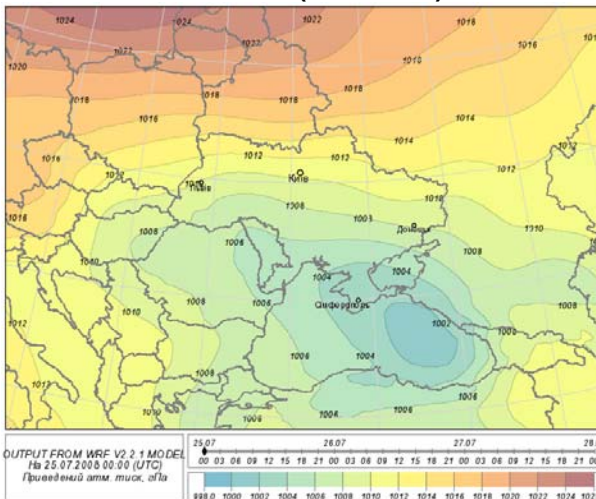
FIG. 2. Surface weather charts.
 The date and time are shown under each from charts of absolute topography.



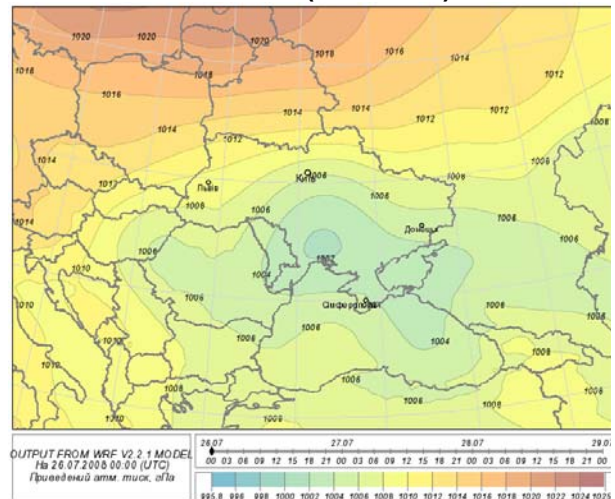
21-Jul-2008 (00.00 UTC)



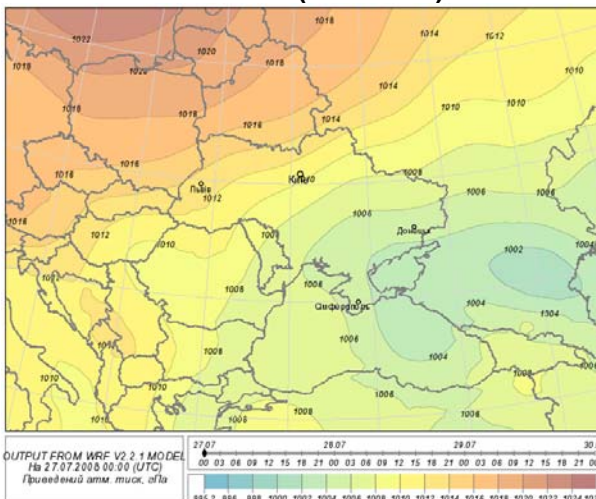
23-Jul-2008 (00.00 UTC)



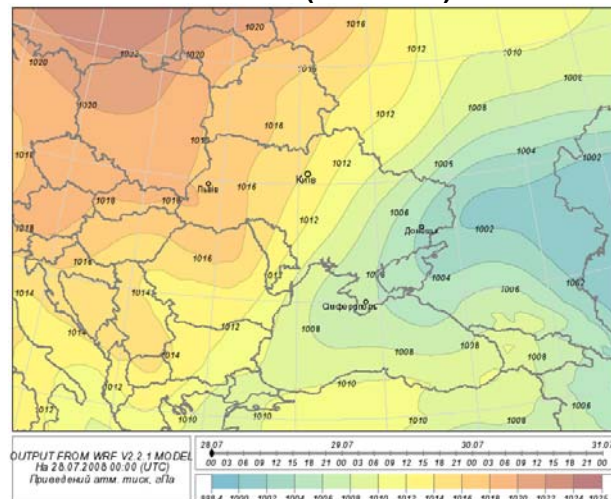
25-Jul-2008 (00.00 UTC)



26-Jul-2008 (00.00 UTC)

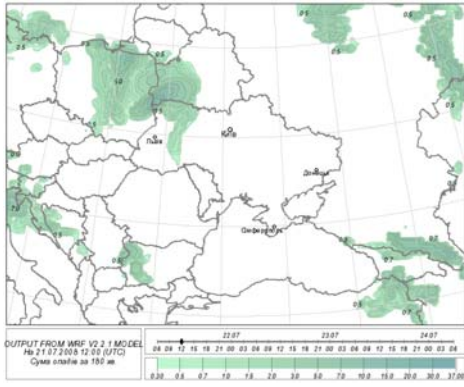


27-Jul-2008 (00.00 UTC)

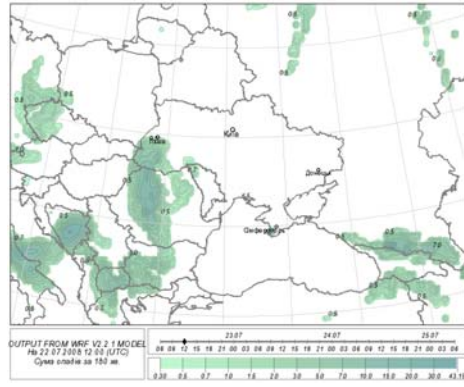


28-Jul-2008 (00.00 UTC)

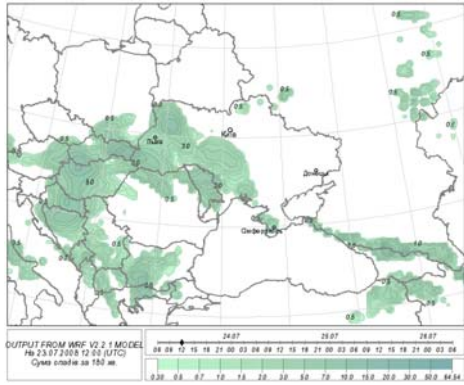
FIG. 3. Sea level pressure (hPa) at time of WRF ARW v.2.2.1 initialization.



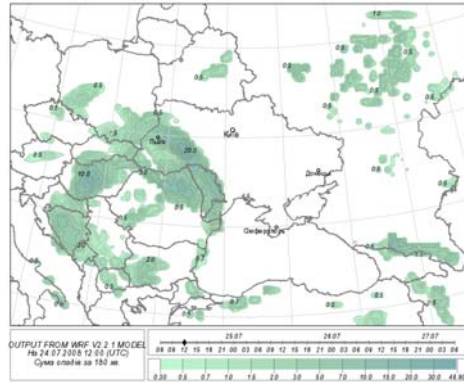
21-Jul-2008 (12.00 UTC)



22-Jul-2008 (12.00 UTC)



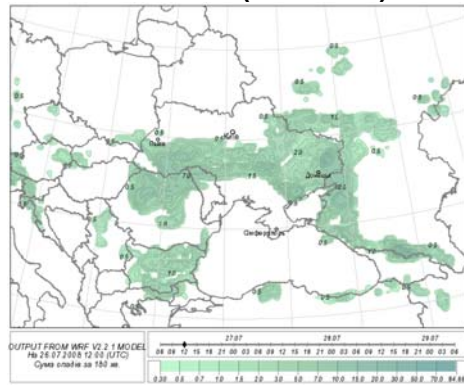
23-Jul-2008 (12.00 UTC)



24-Jul-2008 (12.00 UTC)



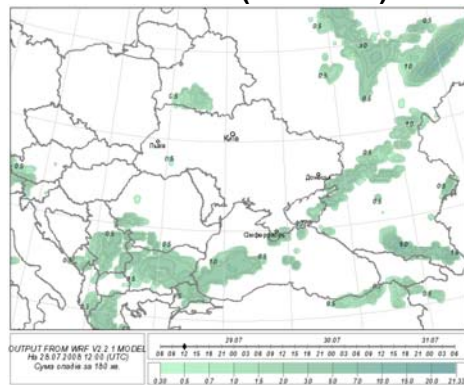
25-Jul-2008 (12.00 UTC)



26-Jul-2008 (12.00 UTC)

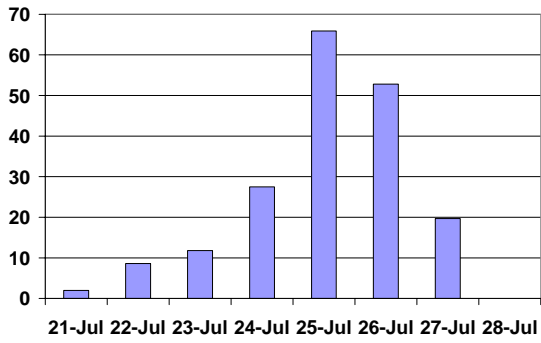


27-Jul-2008 (12.00 UTC)

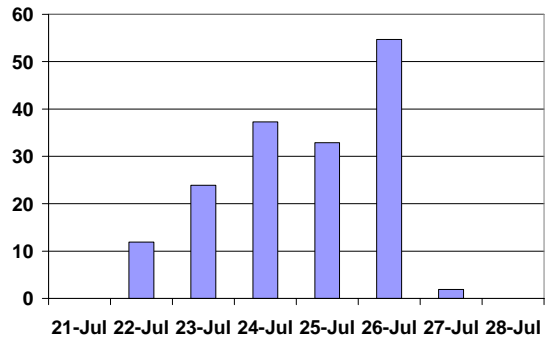


28-Jul-2008 (12.00 UTC)

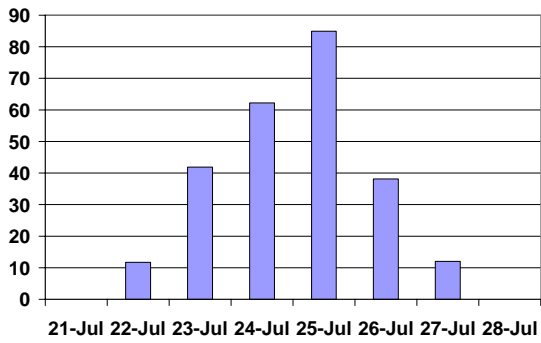
FIG. 4. Precipitation sums (mm/3hour) calculated by WRF ARW v.2.2.1.



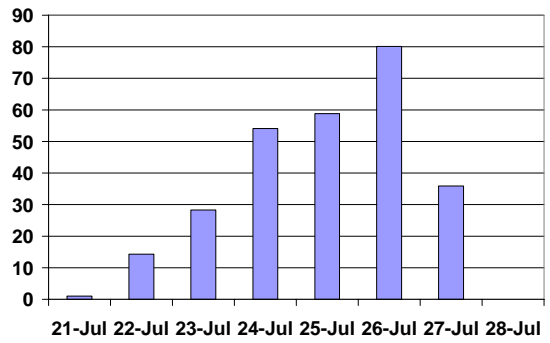
Slavske



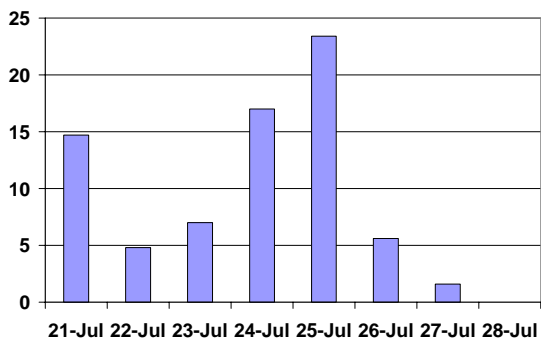
Ivano-Frankivsk



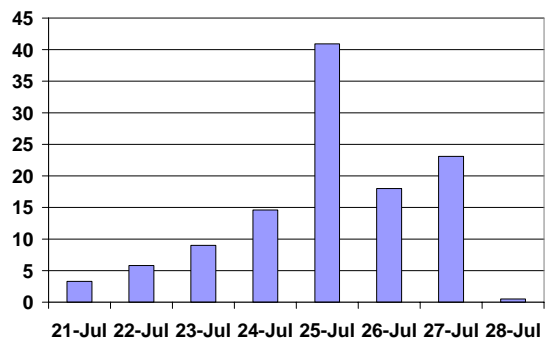
Dolyna



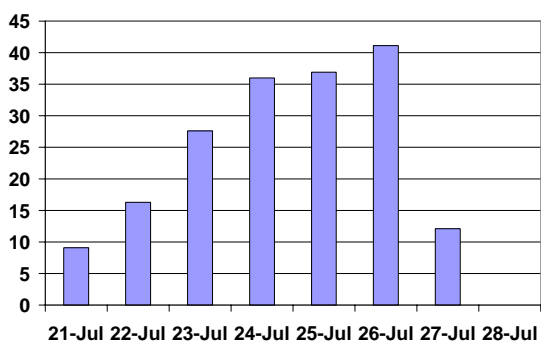
Pozhezhevska



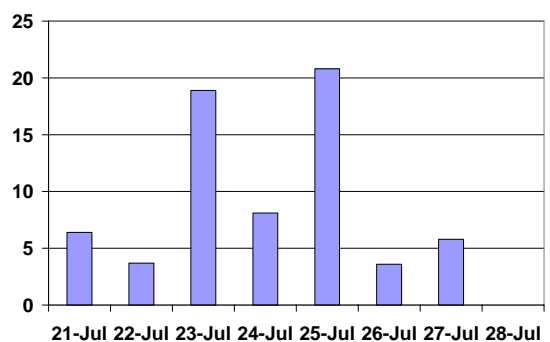
Velykiy Berezniy



Nyzhni Vorota



Plai



Uzhhorod

FIG. 5. Observed precipitation sums from Ukrainian hydrometeorological stations.

Mixed or ice supersaturation layers caused favor condition for heavy and catastrophic precipitation. Such areas have been frequently appeared on 22 and 23 July and rarely did on 21 July.

Calculating of precipitation intensities needs especial attention. Their absolute values are substantially defined by efficiency of cloud and precipitation forming mechanisms.

Numerical experiments have been shown, that change in efficiencies of precipitation forming mechanisms can change their intensity on order and more.

Evolution both cloudiness and precipitation for July, 21-23 is displayed on Fig. 7. Assumption that precipitation formation parameters have mean statistical values in according to (Pirnach, 2008) have been used. Coagulation processes between small drops and large drops, and coagulation crystals with cloud drops have been calculated.

We can see from Fig. 7, strongest precipitation were observed for 22 to 23 July and occupied large areas. On July 21-23 precipitation has been heavy in separate regions if precipitation formation mechanism was efficient enough. For instance, we are note two series cumulus cloud displaced to the north from point $(x,y)=(50, 50)$ km on 21.07.08. There is precipitation intensity reached 8 mm/hrs after 6 hrs of cloud development.

On 22 July cloudiness was founded in both north-east Ukrainian Carpathian region and Dniester left coast. Next numerical modeling has shown that in second case precipitation have not been too strong but occupied larger areas. As numerical simulation shown, distinctive moisture inflows defined the heaviest precipitation. The strongest precipitation-forming activity has been observed when distinctive streams were merged into one. Then intensive forming both of vortex and powerful convective clouds sharply increased the probability of heavy precipitation.

Determinant role in precipitation formation over Carpathians have free to sublimation water vapor that caused fast grow of cloud particles by sublimation and coagulation after. Especially, large drops play the crucial role in formation of catastrophic precipitation. Precipitation had a cell structure with distinctively expressed kernels. Intensity in them can reach the catastrophic values.

The probability of catastrophic precipitation sharply increased when the free to sublimation water vapor appears in the vicinity of these cells. Then that vapor is involved into cells, and results in steady growth of both water and ice particles which resulted are in catastrophic precipitation after.

5. EFFECT OF PRECIPITATION FORMATION MECHANISMS ON HEAVY PRECIPITATION EVOLUTION

We have been investigated the following precipitation-forming mechanism: Findajzen-Berzheron mechanisms (transfer of water vapor from drops on crystals, sublimation growth of crystal to precipitating particles with their next falling); condensation growth of droplets and large drops; coagulation growth of rain drops by gravitation coagulation in approach of continuous growth; freezing of drops; granulation of crystals by capturing of cloudy drops. We have supposed the spherical shape for both drops and crystals.

For to construct the initial state for numerical experiments time 2330 UTC of July 23 have been chosen. Sufficiently intensive precipitation have place in next time.

The chosen calculate grids had the following boundaries:

1) $-300 < x < 500$ km, $-500 < y < 500$ km limited the regular grid with step 20 km. $20 < x < 240$ km, $-100 < y < 120$ km limited the nested grid with step 5 km along x and y .

2) $-35 < x < 70$ km, $25 < y < 50$ km limited the part of nested grid represented the Stry river region. The z -step ($0 < z < 11$ km) limited by 150 m.

The calculated state of cloud characteristics after 2 hrs of their development is show on Fig. 8. Sharp heterogeneity in initial distribution has led to formation of separate spots with high temperature gradients that in turn results in both power convective cloud formations and in strong precipitation. At the first 6 hrs of developing the kernel of strong precipitation was revealed in a grid $35 < x < 70$ km, $25 < y < 50$ km that has been chosen for next numerical experiments.

It must be noted, that ice supersaturation comparable with water content occurred in the chosen grid and as well in its vicinities. Mesoscale structure of such supersaturation consists of variously scaled bands and spots. Water clouds have been located mainly over mountains. Ice clouds occupied the more extensive territory, and they advanced onto studied area both from south-west and from northwest and east. The chosen small region has been located in the northwest direction from the large ice cloud formation. The temperature in this area has been lowered in comparison with surroundings. Ascending motions had spot structure both in mountains and near by regions. Cyclonic motions took place on outlying districts of examined small area.

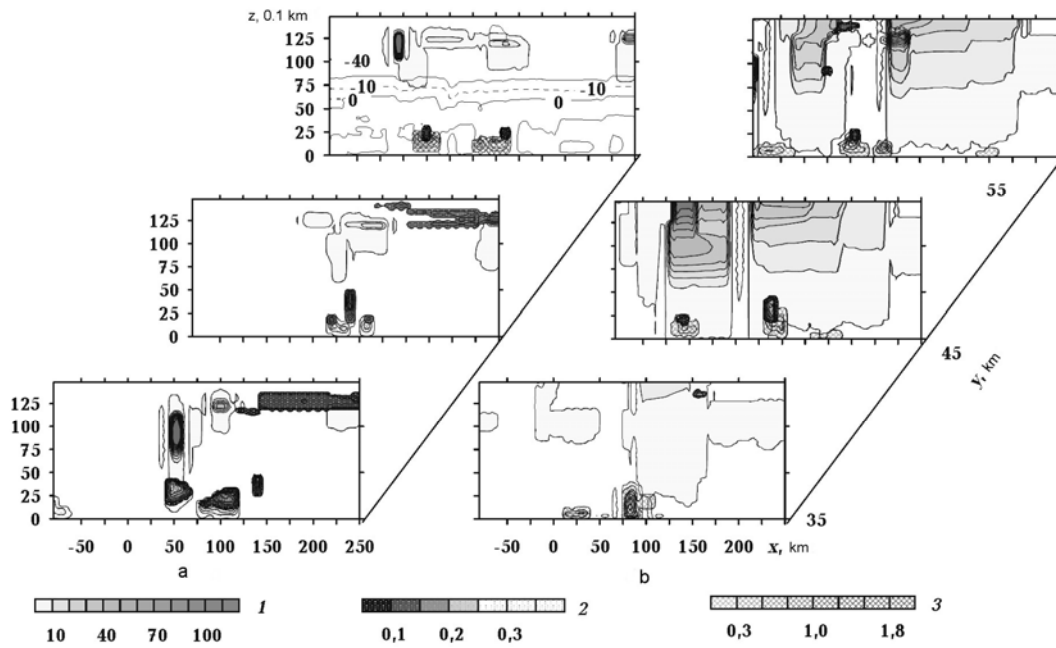


FIG. 6. Spatial distribution of cloud features after 2 hrs of development with various initial atmospheric conditions.

a) 21th of July; b) 23th of July

Numbers near scale: 1) ice concentration, 1/g; 2) ice supersaturation, g/kg; 3) water content, g/kg. Numbers near isolines (fig. 4 a) is temperature.

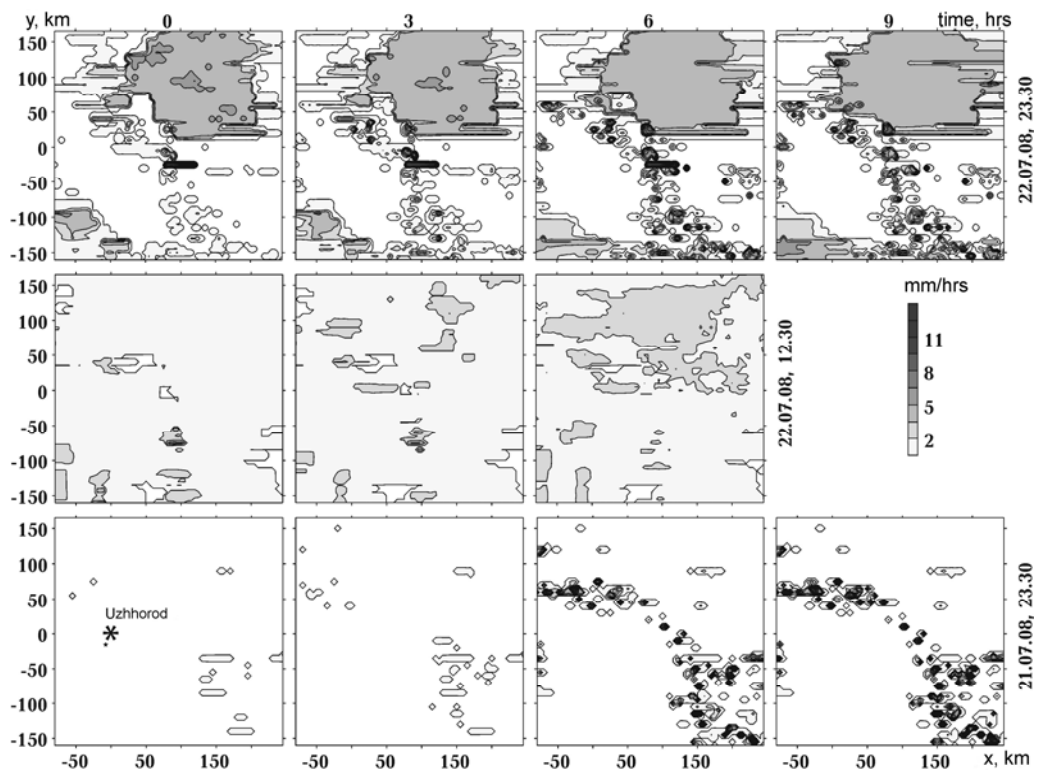


FIG. 7. Evolution of precipitation intensity in July 21-23.

Digits near scale denote the precipitation intensity, mm/hrs; digits on tops are time of cloud development, hrs; data are on the right side. Central point of calculation $(x,y) = (0,0)$ is the Uzhhorod radio sounding station.

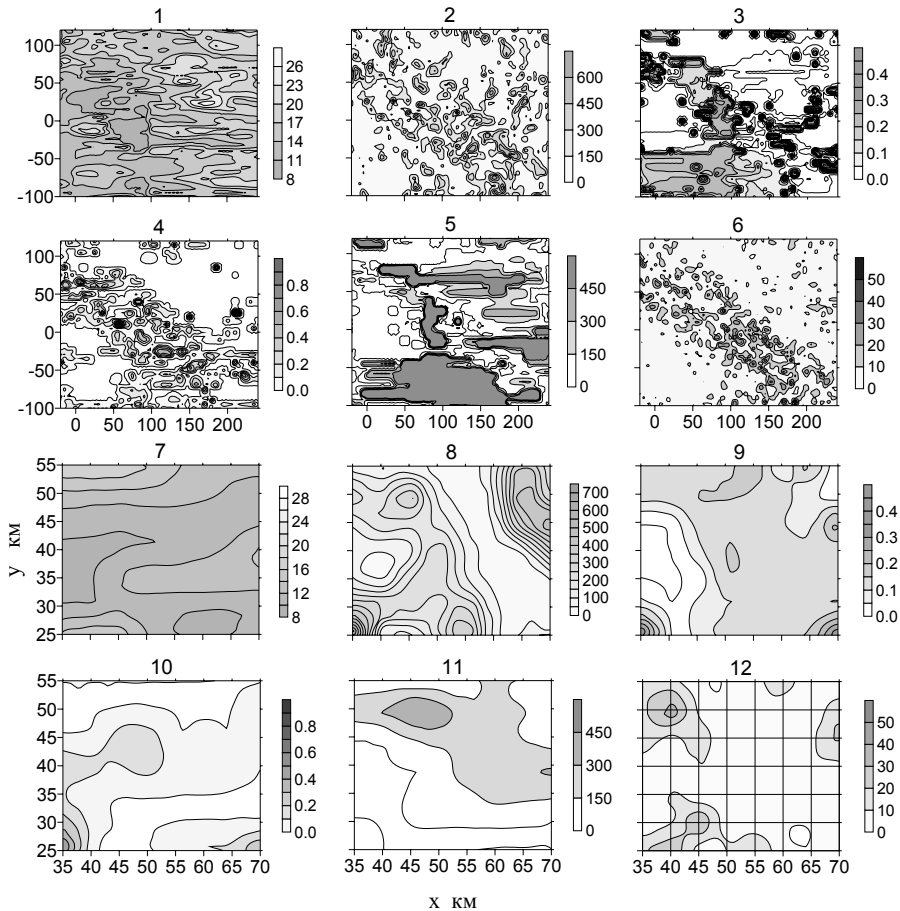


FIG. 8 Spatial distribution of cloud characteristics.

For regular grid (cases 1-6), and for the part of nested grid (cases 7-12) at $t=2$ hrs. 1,7 is the surface temperature, C° ; 2,8 are z – maxima of updrafts, cm/s; 3,9 are ice supersaturation, g/kg; 4,10 are z – maxima of water content, g/kg; 5,11 z – maxima ice concentrations, 1/g; 6,12 are z - maxima of vertical component of cyclonic vortices, $10^{-3}/s$. There have been considered 2, 3, 4 precipitation-forming mechanisms.

Table 1. The maximal sums and intensities of precipitation during 3-6 periods after beginning of cloudiness developing at $35 < x < 70$ km, $25 < y < 50$ km, for various combinations of precipitation-forming mechanisms.

No		1	2	3	4	5	6	7	8	9	10	11
6	\sum_a	39	497	717	39	11	0	0	0	510	40	23
	\sum_d	32	199	717	33	3	0	0	0	182	33	12
J_m , mm/h	3 h	21	166	172	21	2	0	0	0	165	20	2
	6 h	28	317	821	27	25	0	0	0	318	27	35
Combinations		2,4	1,2,4	1,2	2,3,4	1,4	3,4	4	1	1-4	S	E

The note: last line reflects the number of appropriate mechanisms. S is calculated as a column 4, but sublimative intensity is increased; E is calculated as a column 4, $E_0 = 0.1$.

From Fig. 8 (case 11-12) it is seen, that in the top left corner ice clouds with maximal concentrations coincide with cyclonic vorticity. The maximal values of water content coincide with cyclonic vorticity, located in the bottom corner of Fig. 8 (case 10, 12). Such location initiated powerful cumulus cloud developing with the next falling-out of strong precipitation from them.

To illustrate the influence of variously combined precipitation-forming mechanisms on resultant intensities and sum of precipitations, we have been chosen the sums over 3-6 hrs of cloudiness developing, when relative equilibrium established between cloud and precipitation forming processes and falling-out of precipitation. The numerical experiments have been carried out by including or out of the following mechanisms:

1. condensation growth of rain drops;
2. coagulation of rain drops with cloud drops;
3. coagulation of crystals with drops (riming);
4. sublimation growth of ice particles.

Nucleation rate during cloudy evolution can be represented by ratio (Pirnach, 2008)

$$S = 10^{-a} \exp(bT_s)$$

$$b=0,56, a=5.$$

Where T_s is overcooling of air. Coagulating coefficient E_0 was accepted equal 1, except for special case; \sum_a and \sum_d are the total sum of precipitation and part of rain drops, respectively.

The maximal sums on the studied area and the precipitation intensities are presented in Table 1 for the 3-6 hrs period of developing at various combinations of above listed mechanisms.

Numerical experiment results can be divided into 4 categories:

- 1) Precipitation did not fall out at all. These are cases with absence of large drops (cases 6-8 in Table 1.);

- 2) Cases when the sums of precipitation aimed to unlimited value. These are cases with presence both of coagulative processes and condensation of rain drops. Such processes can lead to collapse. There is running of precipitation sums to unlimited value in assistance of great supersaturation with respect both to water and ice (cases 2, 3, 9 in Table 1.);

- 3) Cases, when sums consisted of precipitation, close to strong, or moderate. These are cases in assistance both of sublimative growth of ice crystals and condensative growth of variously sizes rain drops but without coagulation (cases 5,11 in table 1);

- 4) The most stable group with presence of strong precipitation when intensities achieved the catastrophic sizes, but not aimed to unlimited value, in this period the precipitation sums achieved 40 mm/3 hrs. This drop includes computations in assistance of coagulation of large drops with droplets taking into account the presence of ice crystals even at absence coagulation of crystals with drops. Condensation of rain drops either is completely excluded, or needs in special conditions for limitation of its applicability (cases 1, 4, 10 in Table 1).

Modifying of sublimation process by increasing on some order their intensity has not change of precipitation sums. Decreasing intensities of coagulation process results in appreciable decreasing both of precipitation sums and intensities. Especially there is at decreasing of coagulation factor for drops.

Mean over area value of precipitation intensities (Table 2.) has show capability to unlimited growth for cases 2, 3, 9 that include condensation and coagulation growth of large particles. Absence of precipitation is closely associated with absence of large-drops or ice crystal-fractions. Other combination of mechanisms basically provided processes of precipitation formation sufficiently close to reality.

Table 2. Evolution of mean value of precipitation intensities on area $35 < x < 70$ km, $25 < y < 50$ km at various combination of precipitation-forming mechanisms.

№		1	2	3	4	5	6	7	8	9	10	11
6	\sum_a	39	497	717	39	11	0	0	0	510	40	23
	\sum_d	32	199	717	33	3	0	0	0	182	33	12
3	$J_m, \text{ mm/h}$											
	3 h	21	166	172	21	2	0	0	0	165	20	2
	6 h	28	317	821	27	25	0	0	0	318	27	35
Combinations		2,4	1,2,4	1,2	2,3,4	1,4	3,4	4	1	1-4	S	E

Respect to mean values, vertical motion (Table 3) are typical for cumulus cloudiness. Changing of precipitation-forming mechanisms does not change considerably their sizes, but sometimes the differences reached tens in cm/sec. Maximal rate of ascending motions differ significantly for various combinations of mechanisms, thou is difficultly to specify the direct relation between this speeds and precipitation intensities.

For instance, in the case of absent precipitation (cases 6, 7, 8) the maximal values w can differ on 1 m/sec. Their minimal values eventually have been received in assistance only drops in a cloud. Obviously, on that ascending motion are more strongly changed by processes of cloudy condensation and evaporation, that by precipitation falling-out.

Table 3. Updraft, cm/s; min is z-minimums on the area $35 < x < 70$ km, $25 < y < 50$ km; max is z-maxima; mean is presented mean on area value

t, h	As Table 1										
	1	2	3	4	5	6	7	8	9	10	11
3	min	11	15	15	8	8	11	14	15	6	10
	max	558	576	532	580	544	558	545	548	562	466
	mean	139	133	131	147	142	139	131	138	134	124
6	min	9	9	3	8	0	7	9	7	5	9
	max	639	642	676	614	663	765	642	570	660	586
	mean	137	148	148	150	168	162	148	133	151	129

Comparing received results with previous experiments presented in (Palamarchuk and Pirnach, 1992), it is possible to note some distinctions between them. For cold and transitive seasons the main role in the strong precipitation formations play ice particles. In our case role play the large drops, because at their absence strong precipitation did not falled-out. To obtain strong precipitation sufficiently the presence of combination of sublimative growth of crystals and coagulative growth of rain drops.

The account in addition of condensative growth of large drops can lead to the overestimated values of precipitation sums, thou in return they specify for a time and site of possible occurrence of catastrophic precipitation.

6. CONCLUSION

Diagnostic and forecast models have been constructed for mesoscale cloud formations followed by high floods in Carpathian in July, 2008. Numerical experiments are carried out with aim to determine the role of various precipitation-forming mechanisms in formation of strong and catastrophic precipitation.

Relative role of large drop and ice fractions in formation of heavy precipitation was defined.

It is found, the unlimited growth of water and ice supersaturation is possible if mechanisms of cloud precipitation formation are insufficiently effective for precipitating of whole moisture. In turn, it can cause intensive

activation of cloud condensation nuclei and unlimited growth of large drops as well. Therefore the unlimited growth of precipitation intensities may occur.

Some key parameters, meteorological conditions and predictors caused the occurrence of dangerous phenomena were defined.

The main features of strong precipitation have been noted as follows:

- 1) interaction of flows of different physical nature coming from opposite directions;
- 2) presence of ice supersaturation layers;
- 3) strong vortical motions in single air mass advanced to mountain ridge;
- 4) chimney clouds with ice tops and cirrus clouds above;
- 5) high tropopause achieved 10 km and more, strong ascending and compensative descending motions with velocities ≥ 10 m/s;
- 6) the necessary combination of precipitation-forming mechanisms.

7. REFERENCES

- Boyko, V.M., Kulbida, M.I., and M.M. Susidko, 1999: A famous rain flood on the rivers of Zakarpattya region in November of 1998. *Trudy UHMI*, **247**, 91-101 (In Ukrainian).
- Kasahara, A., 1974: Various vertical coordinate systems used for numerical weather prediction. *Mon. Wea. Rev.*, **102**, 509-522.
- Marshall, J. S. and W. Mc K. Palmer, 1948: The distribution of raindrops with size. *Journal of Meteorology*, **5**, 165-166.

- Palamarchuk, L., Pirnach, A.M., 1992. Study of an internal structure of frontal zone with the help of three-dimensional numerical models. *Trudy UHRI*, **243**, 107–125 (In Russian).
- Pirnach, A.M., 1998. Construction and application of the various numerical models for study the cloud dynamics and structure of the frontal rainbands. *Atmos. Res.* 45-47, 355-376.
- Pirnach, G.M., 2004: Modeling of frontal clouds with heavy precipitation for plates and mountains relief. *Trudy UHMI*, **253**, 37-50 (In Ukrainian).
- Pirnach, G.M., 2007: Modeling of evolution of mesoscale cloud formations over Carpathian. *Trudy UHMI*, **256**, 19-43 (In Ukrainian).
- Pirnach, G.M., 2008: Numerical modeling of clouds and precipitation in atmospheric frontal systems. Kyiv, Nika-Center, 294 pp.
- Pirnach, G.M., Dudar, S.M., and V.M. Shpyg, 2006: Numerical modeling of the frontal cloud systems which accompanied a strong flood in Carpathians in November 1998. *Trudy UHMI*, **255**, 5-24 (In Ukrainian).
- Pirnach, A.M. and S.V. Krakovskaya, 1994: Numerical studies of dynamics and cloud microphysics of the frontal rainbands. *Atmos. Res.*, **33**, 333-365.
- Pirnach, G.M., Zabolocka, T.M., Pidgurska, V.M., and T.M. Shpytal, 2002: Numerical and experimental researches of the frontal systems which caused the dangerous phenomena over Ukraine. *Trudy UHMI*, **250**, 42-60 (In Ukrainian).
- Shyshkin, N.S., 1964: Clouds, precipitation and thunderstorm electricity. Leningrad, Hydrometeorological Publishing Center, 404 pp.